ELSEVIER

Biochemical Engineering Journal 29 (2006) 109–118

Biochemical Engineering Journal

www.elsevier.com/locate/bej

Simulation and real-time monitoring of polymerase chain reaction for its higher efficiency

Ji Youn Lee [a,1], Hee-Woong Lim [b,1], Suk-In Yoo [b], Byoung-Tak Zhang [b], Tai Hyun Park [a,*]

[a] *School of Chemical and Biological Engineering, Seoul National University, San 56-1, Shillim-dong, Gwanak-gu, Seoul 151-744, Republic of Korea*
[b] *School of Computer Science and Engineering, Seoul National University, San 56-1, Shillim-dong, Gwanak-gu, Seoul 151-744, Republic of Korea*

Received 15 October 2004; accepted 25 February 2005

Abstract

Polymerase chain reaction (PCR) is an important molecular biological tool for the amplification of nucleic acids. PCR process can be divided into three phases according to the amplification rate: exponential, quasi-linear, and plateau. We investigated the cause of the plateau phenomenon through real-time monitoring of the amplification profile and computerized simulation. Possible limiting components, such as *Taq* DNA polymerase, primer pair, and dNTPs were added during quasi-linear phase, after which the differences in the amplification profiles were monitored. Modeling and computerized simulations were performed to look into the complex mechanism of the reactions, such as renaturation of templates during temperature transition from denaturation to annealing step and effective enzyme concentration profiles within the cycle progress. The decrease of effective polymerase concentration due to heat inactivation and product accumulation caused the PCR plateau. Addition of polymerase during the quasi-linear phase could increase the final product amount; however, the PCR process still reached the plateau phase in spite of polymerase addition. Simulation results suggest that renaturation of templates before competitive annealing reaction and decrease of effective enzyme concentration by non-specific binding of polymerase to double-stranded DNA is the main contribution to plateau forming.

Keywords: Bioreactions; DNA; Enzyme inactivation; Modeling; Polymerase chain reaction (PCR); Plateau

1. Introduction

Polymerase chain reaction is an in vitro DNA amplification method that was introduced in 1985 [1]. The process was automated by the adoption of the thermostable *Taq* DNA polymerase [2]. PCR is an essential molecular biological tool, because it can amplify tiny amount of DNA. Many biochemical tools, such as sequencing to read out the sequence of DNA strand, RT-PCR to quantify the amount of transcribed mRNA, DNA shuffling for in vitro evolution, and allele-specific PCR to find out the polymorphism of human can all be achieved by virtue of PCR. Recently, PCR is miniaturized and integrated with other analytical techniques for various applications [3–5].

Theoretically, the target DNA is doubled every cycle, and consequently the amount of DNA increases exponentially. However, the efficiency drops abruptly after 10–20 cycles which varies according to the initial template amount and decreases to nearly zero in the later cycles. The latter phenomenon is called plateau, which is an attenuation of amplification rate. Factors such as substrates consumptions, active polymerase concentration decrease, and renaturation of products have been presumed to contribute this phenomenon [6,7]. The factors that lead to plateau are also important parameters affecting amplification efficiency. Analysis of PCR plateau phenomenon can provide a deeper insight of the PCR mechanism.

Many studies about PCR have been performed in mathematical as well as in experimental approaches. In some studies, PCR process was formulated as a deterministic process [8–11]. The attenuation of amplification efficiency by the limitation of polymerase was modeled [10],

* Corresponding author. Tel.: +82 2 880 8020; fax: +82 2 875 9348.
E-mail address: thpark@plaza.snu.ac.kr (T.H. Park).
[1] Both authors contributed equally to this work.

1369-703X/$ – see front matter © 2005 Elsevier B.V. All rights reserved.
doi:10.1016/j.bej.2005.02.023

Nomenclature

$C_{ds,t}$	concentration of dsDNA at t second in each step (M)
C_{enz}	active polymerase concentration reflecting thermal inactivation (M)
$C_{hd,t}$	concentration of primer-template hetero duplex at t second in each step (M)
C_m	template concentration of a given melting profile (M)
$C_{p,t}$	concentration of primer at t second in each step (M)
$C_{ss,t}$	concentration of ssDNA at t second in each step (M)
dsDNA	double-stranded template DNA
E_a	annealing efficiency
E_d	denaturation efficiency
E_e	extension efficiency
f_{ss}	ratio of denatured template
hdDNA	primer-template hetero duplex
k_{a1}	rate constant of annealing between primer and template strand ($M^{-1}\,s^{-1}$)
k_{a2}	rate constant of renaturation between complementary template strands ($M^{-1}\,s^{-1}$)
K_d	dissociation equilibrium constant of template DNA (M)
$k_{e,t}$	rate constant of extension at t second in extension step ($M^{-1}\,s^{-1}$)
k_{nu}	nucleotide incorporation rate of primer single-stranded primers (both forward and backward)
l, l_p	template length and primer length (mer)
primer	single-stranded primers (both forward and backward)
ssDNA	single-stranded template DNA
t	time, reset to zero at the beginning of each step (s)
T, T_m	temperature and melting temperature (°C) *Taq* polymerase (nucleotide/s molecule)

Greek letter

α_t	effective polymerase ratio at t second in extension step

and enzyme binding/elongation process was formulated using Michaelis–Menten equation [8,9]. Various stochastic approaches were also performed. PCR amplification was modeled as a result of branching process including mutation in extension [12,13]. Velikanov et al. focused on the microscopic mechanism of dNTP incorporation in the extension step and modeled it as a Markov process [14]. A model combining deterministic and stochastic approaches was also suggested by Stolovitzky and Cecchi [15]. In this model, mass-action equations to calculate amplification efficiency were applied and the PCR process was modeled with a branching process. Recently, Whitney et al. reported a model that applied a competitive hybridization in the annealing step using mass-action equation and calculated extension efficiency considering a competition among dNTPs and pyrophosphate [16].

In this paper, we focused on the factors that lead to PCR plateau and investigated the addition effect of each component on the amplification profile. Then, we developed a mathematical model of the PCR process based on the deterministic approach, which describes three steps (i.e. denaturation, annealing, and extension), respectively. The changes of PCR substrates and intermediates, and the efficiencies at each step were presented by computer simulation. Based on those results, we analyzed the cause of the PCR plateau and other parameters influencing the PCR efficiency.

2. Materials and methods

2.1. PCR mixture preparation

Two DNA templates strands were prepared for PCR amplification. *β-actin* fragment (159 bp) was obtained by RT-PCR from HL-60 cell and *30Kc12* gene (795 bp) was obtained by RT-PCR from *Bombyx mori*. Each PCR product was purified by gel elution and quantified spectrophotometically. The sequences of forward and backward primers for *β-actin* fragment were 5′-GACTTAGTTGCGTTACACCCTTTC-3′ and 5′-GCTGTCACCTTCACCGTTCC-3′, respectively. The sequences of forward and backward primers for *30Kc12* were 5′-CCTGAATTCATGAAACTTCTCGTTGTG-3′ and 5′-TTTGAATTCTTAGAAAGGTGTAATGAACC-3′, respectively. For the PCR mixture preparation, iQ SYBR® Green Supermix (Bio-Rad, CA, USA), 0.2 μM of each primer, appropriate amount of template and distilled water were mixed to 20 μl. The 2X SYBR® Green Supermix contains 100 mM KCl, 40 mM Tris–HCl, pH 8.4, 0.4 mM of each dNTP, 50 units/ml iTaq polymerase, 6 mM $MgCl_2$, SYBR Green I, 20 nM fluoresscein, and stabilizers.

2.2. Addition of PCR components

To monitor the effect of the added components, 1.24×10^{-14} M *β-actin* fragment and 4.94×10^{-14} M of *30Kc12* were used as templates. During quasi-linear phase, 0.2 μl of *Taq* polymerase (5 units/μl), primer pair (each 10 μM), dNTPs mixture (each 10 mM), SYBR Green I (50× solution), or mixture of them were added to each tube. For a control sample, equal volume of distilled water was added.

2.3. Real-time monitoring of amplification profile

The reaction mixture was first denatured for 1 min at 94 °C, followed by 35 cycles consisting of 20 s at 94 °C for denaturation, 15 s at 55 °C for annealing, and 30 s at 72 °C for extension. The accumulated PCR product was measured by

measuring the fluorescence emission from SYBR Green I dye in the extension step. The PCR was carried out in 0.2 ml PCR plate using an iCycler iQ instrument (Bio-Rad, CA, USA) and analysis was achieved using an iCycler iQ software version 3.0.

2.4. PCR product analysis

The PCR products were analyzed by melting curve measurement and gel electrophoresis. Agarose gel electrophoresis was performed with 1% (for *β-actin* fragment) or 2% (for *30Kc12*) UltraPure™ Agarose (Invitrogen, CA, USA) in 0.5× Tris–acetate–EDTA buffer and the gel was stained with ethidium bromide. As a size marker, GeneRuler™ 50 bp DNA ladder (Fermentas, MD, USA) was used and was also used as a standard for quantification. The gel image was obtained with a Gel-Doc and analyzed by Quantity One™ (Bio-Rad, USA).

3. Model development

One cycle of PCR consists of three steps, including the enzymatic reaction of polymerase. The efficiency in each cycle is influenced by many complex factors, which are reflected in one parameter, i.e. the amplification yield in each cycle. Parameters affecting the efficiency of PCR are as follows: concentrations of template DNA, DNA polymerase, dNTPs, $MgCl_2$, and primers; denaturation, annealing and extension temperatures; time of each step; number of cycles; temperature ramping rates and the presence of contaminating DNA and inhibitors in the sample. However, we do not need to consider them all, since the impact of the factors differs and the controllable parameters of the process are limited. In this section, we will describe a mathematical model, which consists of denaturation, annealing, and extension.

3.1. Denaturation step

Template DNA dissociates into two single-stranded DNA molecules (Watson and Crick strands) in the first step of the cycle, and the reaction can be written as follows:

$$\text{dsDNA} \overset{k_d, k_d^{-1}}{\longleftrightarrow} \text{ssDNA}_1 + \text{ssDNA}_2 \tag{1}$$

Usually, denaturation is carried out at 94–95 °C which is the highest temperature for enzyme activity, and high enough for DNA molecules to exist in a single-stranded form. Therefore, usually denaturation efficiency is considered the unity and only annealing or extension efficiencies are considered [10,14,15]. However, the denaturation step at lower temperature may be required for a specific purpose [17], and in this case, the denaturation efficiency can be obtained from a melting profile of a known template concentration.

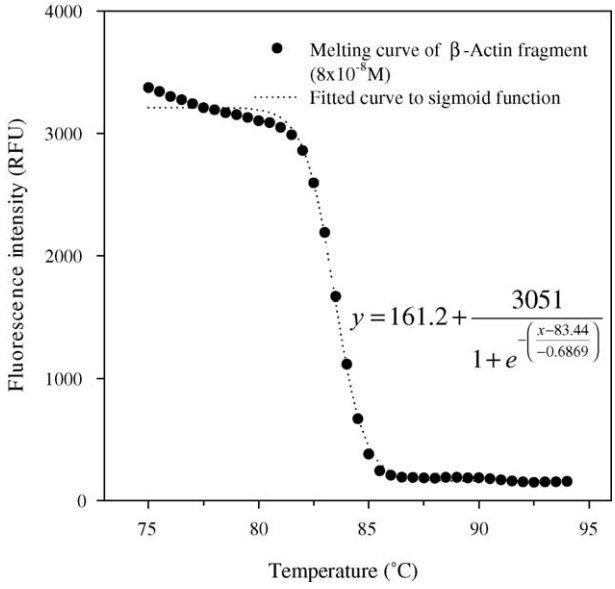

Fig. 1. Melting curve of *β-actin* fragment (8×10^{-8} M) that was obtained with iCycler iQ™ real-time PCR machine and its sigmoid fitted curve.

A typical DNA melting curve of homogeneous solution is sigmoidal, so the melting curve can be fitted to as follows:

$$f_{ss}(T) = \frac{1}{1 + e^{-a(T - T_m)}} \tag{2}$$

where a is the transition width of the curve. An example of a melting curve and the fitted sigmoid curve is shown in Fig. 1. Assuming that the reaction is in equilibrium at each temperature in melting profile, the equilibrium constant of template dissociation (K_d) can be calculated at any temperature as follows:

$$K_d(T) = \frac{k_d}{k_d^{-1}} = \frac{(f_{ss}(T)C_m)^2}{(1 - f_{ss}(T))C_m} \tag{3}$$

Denaturation efficiency (E_d) can be calculated from the above equation and the template dsDNA concentration ($C_{ds,0}$) at the beginning of denaturation step as follows:

$$E_d = \frac{C_{ds} - C_{ds,0}}{C_{ds,0}} = \frac{-K_d(T) + \sqrt{K_d(T)^2 + 4K_d(T)C_{ds,0}}}{2C_{ds,0}} \tag{4}$$

If we assume that the Watson and Crick strands have identical properties, common notations for the reactions of the Watson template and Crick template in differential equations can be applied to subsequent steps. The concentration of the denatured template can be calculated from Eq. (4), and is used as input of the following annealing step.

3.2. Annealing step

In the annealing step, denatured template strands hybridize with primers to form primer-template hetero duplexes or

the denatured templates renature to form double-stranded templates. Usually, the renaturation reaction between complementary templates is thermodynamically more favorable, therefore excess amount of primers are used (order of magnitude: 4–8) to promote the generation of primer-template hetero duplexes. Hybridization between complementary DNA can be characterized with two parameters: equilibrium yield and annealing rate [18]. If a sufficient incubation time is assumed, the equilibrium yield is the main consideration. On the other hand, if the competition between DNA strands is important, the annealing rate becomes the main consideration. The annealing step in PCR is a competitive reaction between templates and primers, so the annealing rate is an important factor in deciding the annealing efficiency.

Moreover, the transition time from denaturation temperature (usually 94–95 °C) to annealing temperature (normally 50–60 °C) is not negligible when using conventional thermocyclers. Considering a cooling rate of 1 °C/s, which is a common cooling rate of thermocyclers utilizing a Peltier heating element and microtiter plate, the transition time is about 30–40 s. During the temperature transition, renaturation between template strands takes place before competitive annealing, which is called pre-annealing. Pre-annealing is assumed to occur during the temperature transition between the melting temperature of template and that of primer.

Two hybridization reactions that occur in annealing step are

$$\text{primer}_1 + \text{ssDNA}_1 \xrightarrow{k_{a1}} \text{hdDNA}_1 \tag{5}$$

$$\text{primer}_2 + \text{ssDNA}_2 \xrightarrow{k_{a1}} \text{hdDNA}_2 \tag{6}$$

$$\text{ssDNA}_1 + \text{ssDNA}_2 \xrightarrow{k_{a2}} \text{dsDNA} \tag{7}$$

and the reaction (7) takes place only in pre-annealing. The annealing temperature is much lower than the melting temperatures of template and primer. Therefore, the equilibriums are shifted to the formation of double-stranded DNA while the reverse reactions, dissociations are negligible. Pre-annealing and competitive annealing can be formulated by the following differential equations.

Pre-annealing:

$$\frac{dC_{ds,t}}{dt} = k_{a2}(C_{ss,0} - C_{hd,t} - C_{ds,t})^2 \tag{8}$$

$$C_{ds,0} = 0 \tag{9}$$

Competitive annealing:

$$\frac{dC_{hd,t}}{dt} = k_{a1}(C_{pr,0} - C_{hd,t})(C_{ss,0} - C_{hd,t} - C_{ds,t}) \tag{10}$$

$$\frac{dC_{ds,t}}{dt} = k_{a2}(C_{ss,0} - C_{hd,t} - C_{ds,t})^2 \tag{11}$$

$$C_{hd,0} = 0 \tag{12}$$

In the above equations, the initial condition for $C_{ds,t}$ in competitive annealing is set to be the result of pre-annealing, and t is the reset to zero at the beginning of each reaction.

The hybridization rate constant (k) is known to be related with the strand lengths:

$$k \propto \frac{\sqrt{L}}{N} \tag{13}$$

where L and N denote primer length and template complexity (i.e. length of the template), respectively. Assuming that annealing time is sufficient, the remaining single-stranded template after annealing step is negligible, therefore the annealing efficiency can be calculated from the above Eqs. (8)–(12) and the ratio of rate constants, k_{a1} and k_{a2}. In the simulation, the annealing efficiency (E_a) is defined by the following equation:

$$E_a = \frac{C_{hd}}{C_{ss,0}} \tag{14}$$

3.3. Extension (polymerization) step

Extension is the most complicated step in describing the mathematical equations, because it consists of tens of reactions including polymerase binding, dNTP incorporation, deformation of the complex, and polymerase detachment. It is impossible to represent all these details and a sub-reaction in dNTP incorporation is known as the rate determining step. Therefore, dNTP incorporation has been considered as the main factor and has been modeled as stochastic process like Markov chain [14] or mass-action equation like Michaelis–Menten equation [8,9]. In our model, we focused on the effect of limited amount of polymerase. We assumed optimized buffer condition, no partial extension, and negligible dNTP incorporation error during elongation.

Polymerase incorporates the dNTPs to the hetero duplexes formed in the previous step and elongates them to the double-stranded DNA product. Hence, effective amount of polymerase plays a critical role in the extension step. In the early cycles of PCR, the amount of polymerase (1–2 nM) is sufficient in comparison to the concentration of hetero duplex molecules (10^{-2} to 10 pM), and therefore most hetero duplexes are converted to a complete duplex. However, as the cycle progresses, amplified template concentration exceeds polymerase concentration and hetero duplexes will remain that are not bound by polymerase. Hsu et al. developed a kinetic model that considered the dNTP incorporation rate of polymerase to reflect the limitation of polymerase [10] and we extended the model to consider polymerase binding probability.

The reaction can be written as follows:

$$\text{hdDNA} \xrightarrow{k_{e,t}} \text{dsDNA} \tag{15}$$

The reaction rate ($k_{e,t}$) depends on the amount of polymerase, therefore, the differential equation for the above reaction and $k_{e,t}$ are

$$\frac{dC_{ds,t}}{dt} = k_{e,t} \tag{16}$$

$$k_{e,t} = \frac{k_{nu}}{l - l_p} C_{enz} \alpha_t \tag{17}$$

Taq polymerase lacks binding-specificity so they can bind any kind of double-stranded DNA [19]. The amount of double-stranded DNA increases with each cycle, so the effective polymerase concentration must be calculated considering both concentrations of double stranded template and hetero duplex. Assuming that polymerase binding ratio is proportional to the duplex length, the effective polymerase ratio, α_t can be expressed as follows:

$$\alpha_t = \frac{l_p C_{hd,t}}{l_p C_{hd,t} + l C_{ds,t}} \tag{18}$$

From Eqs. (16)–(18), we can rewrite the rate equation for double stranded template to the following equation:

$$\frac{dC_{ds,t}}{dt} = \frac{k_{nu}}{l - l_p} C_{enz} \frac{l_p (C_0 - C_{ds,t})}{l_p C_0 + (l - l_p) C_{ds,t}} \tag{19}$$

with

$$C_0 = C_{hd,t} + C_{ds,t} = C_{hd,0} + C_{ds,0} \tag{20}$$

and extension efficiency E_e is defined as

$$E_e = \frac{C_{ds} - C_{ds,0}}{C_{hd,0}} \tag{21}$$

where C_{ds} is double stranded template concentration at the end of extension step. The extension results are calculated numerically.

3.4. Thermal inactivation of Taq polymerase

It is known that the inactivation of *Taq* DNA polymerase follows a first order reaction [20,21]. Therefore, we calculated the Arrhenius constant and energy of inactivation using half life data like in the Hsu's work [10]. The thermal inactivation of enzymes was considered not only in the denaturation step but also in the other steps and intervals. Enzyme inactivation is calculated numerically.

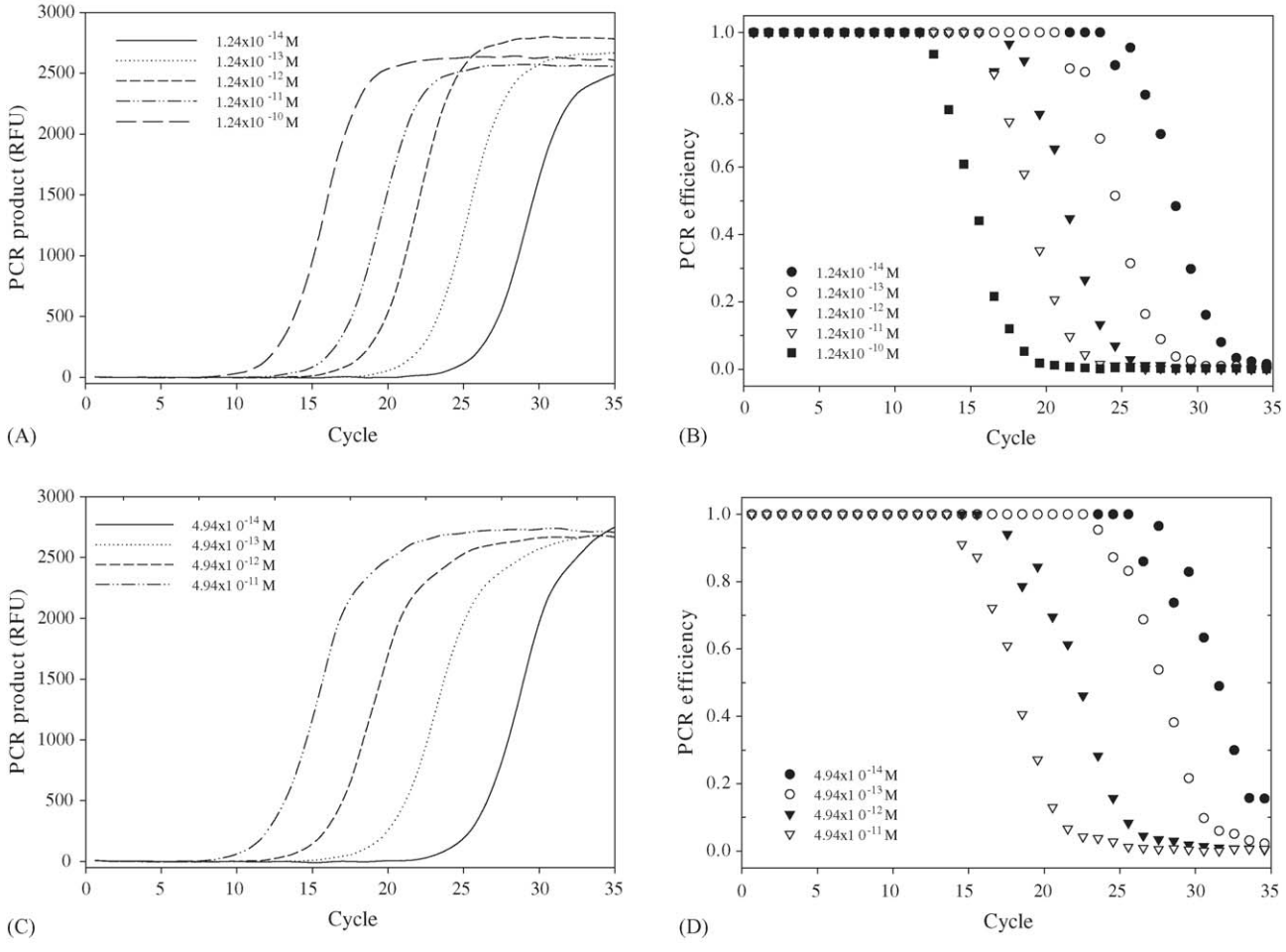

Fig. 2. Real-time amplification monitoring results. (A) Amplification profile of serially diluted templates (*β-actin* fragment). (B) PCR efficiency profile (*β-actin* fragment). (C) Amplification profile of serially diluted templates (*30Kc12*). (D) PCR efficiency profile (*30Kc12*).

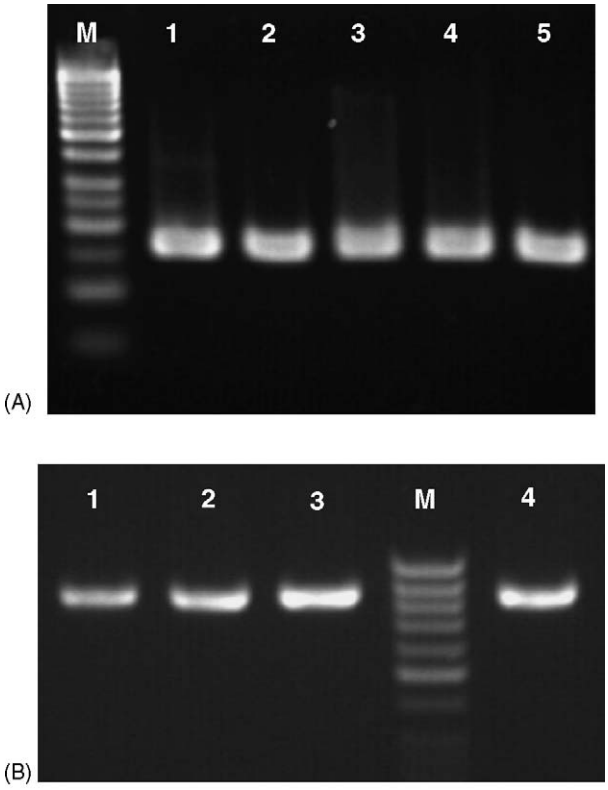

Fig. 3. Agarose gel electrophoresis results of PCR products of serially diluted templates. (A) *β-actin*, M denotes marker (50 bp ladder). Lanes 1–5 are the PCR products of different initial template concentrations (from 1.24×10^{-10} M to 1.24×10^{-14} M, serial 10-fold dilution). (B) *30Kc12*, lanes 1–4 are the PCR products of different initial template concentrations (from 4.94×10^{-11} M to 4.94×10^{-14} M, serial 10-fold dilution).

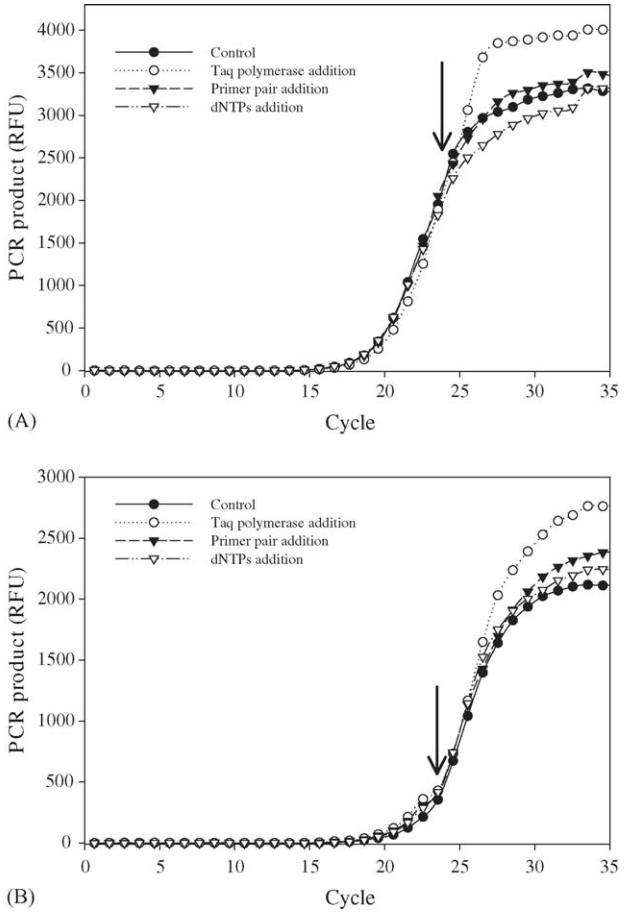

Fig. 4. Effect of PCR components addition on amplification profile. (A) *β-actin* fragment (B) *30Kc12*. (●): control (distilled water addition), (◯): *Taq* polymerase addition, (▼): primer pair addition. (□): *Taq* polymerase and primer pair addition. The arrows indicate the cycle when the components were added.

4. Results and discussion

4.1. Amplification profile of serially diluted templates

Amplification profiles of serially diluted templates are shown in Fig. 2. Regardless of the initial template concentration and length, they show typical PCR amplification profiles which consists of exponential, quasi-linear, and plateau phases. Though the plateau starting cycle was increased according to the dilution of templates, obvious plateau phases were observed. PCR efficiency dropped abruptly after 10–20 cycles. After passing through 14–18 cycles of quasi-linear phase, the PCR process finally entered the plateau phase. Final PCR products were electrophoretically separated and analyzed (Fig. 3). The final amounts were about 8–9 ng/μl for *β-actin* fragment and 4.5–5.5 ng/μl for *30Kc12*, corresponding to $8–9 \times 10^{-8}$ M and $0.9–1 \times 10^{-8}$ M, respectively.

4.2. Addition of PCR components

Several components were added during the PCR process to check if they are limiting parameters or not. So we chose possible components of PCR such as *Taq* polymerase, primer pair, and dNTPs, which are usually user-optimized and can be readily added. Each component was added solely or mixed with other components. Reporter dye molecule, SYBR Green I, was also added with other additives to check if the plateau in real-time monitoring was due to dye limitation.

The initial polymerase concentration in PCR mixture was 2 nM, and the same amount of polymerase was added after 23 cycles of amplification. The addition brought a fluorescence intensity increase as shown in Fig. 4; however the signal difference was not significant as expected. Therefore, the PCR products were subjected to electrophoresis and analyzed. According to image analysis result, the amount of PCR products to which polymerase was added was twice as much as the control sample (lanes 1, 4 and 5 in Fig. 5). Probably the fluorescence intensity in the later cycle was underestimated because the dye molecules were not sufficient as to be proportion to the PCR product amount. The reporter dye molecule addition induced the increase of fluorescence intensity; however, the tendency of the amplification profile did not change and also the plateau phase appeared regardless of the addition of dye molecules.

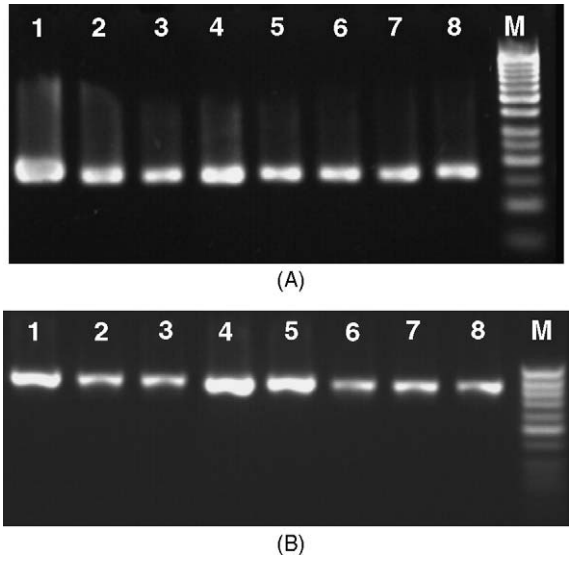

Fig. 5. Agarose gel electrophoresis results of PCR products. (A) *β-actin* fragment. (B) *30Kc12*, M denotes marker (50 bp ladder). Lane 1: *Taq* polymerase addition; lane 2: primer pair addition; lane 3: dNTPs addition; lane 4: *Taq* polymerase and primer pair addition; lane 5: *Taq* polymerase and SYBR Green I addition; lane 6: primer pair and SYBR Green I addition; lane 7: dNTPs and SYBR Green I addition; lane 8: control (distilled water addition).

Primer depletion in the later cycle is thought to be suspicious because the excess of primer to template order of magnitude 4–8 decreased to 1–2, where after consequently, the primer-template hetero duplex formation is reduced. Primer pair addition showed a slight increase both in fluorescence intensity and in the final amount of PCR product (Fig. 4 and lanes 2 and 6 in Fig. 5). Though the addition of primer pair can increase the final product amount, the increase was not as significant as the addition of polymerase, while the plateau phase was still observed.

Addition of dNTPs showed no significant change both in the amplification profile and in final PCR product amount as shown in Fig. 4 and lanes 3 and 7 in Fig. 5. *Taq* polymerase and primer pair were added together, but they did not give noticeable synergistic effect compared to addition of polymerase only (lane 4 in Fig. 5).

4.3. Simulation results I: addition of PCR components

The addition of key components influencing the PCR efficiency, such as *Taq* polymerase and primer pair contributed to the final product amount increase. However, the plateau phase was still observed. To investigate the mechanism inside of the complex reaction, we performed a simulation based on the model developed in Section 3. Simulation was executed with *β-actin* fragment under same condition as the experiment.

With the simulation we could track the changes of substrates and intermediates formed during the reaction. We focused on two sub-reactions and their reactants and products profiles to explain the phenomenon mentioned above. One was the pre-annealing reaction which was caused by the renaturation of templates during temperature transition from denaturation to annealing. As template accumulated, the pre-annealing ratio and renaturation in competitive annealing also increased. The other was the decrease of extension efficiency which was caused by the deficiency of active enzyme and a non-specific binding property of *Taq* polymerase. Concentration of effective enzyme decreased with PCR progress because of thermal inactivation and product accumulation. Therefore, product accumulation could affect both annealing efficiency and extension efficiency and consequently lead to the plateau phase.

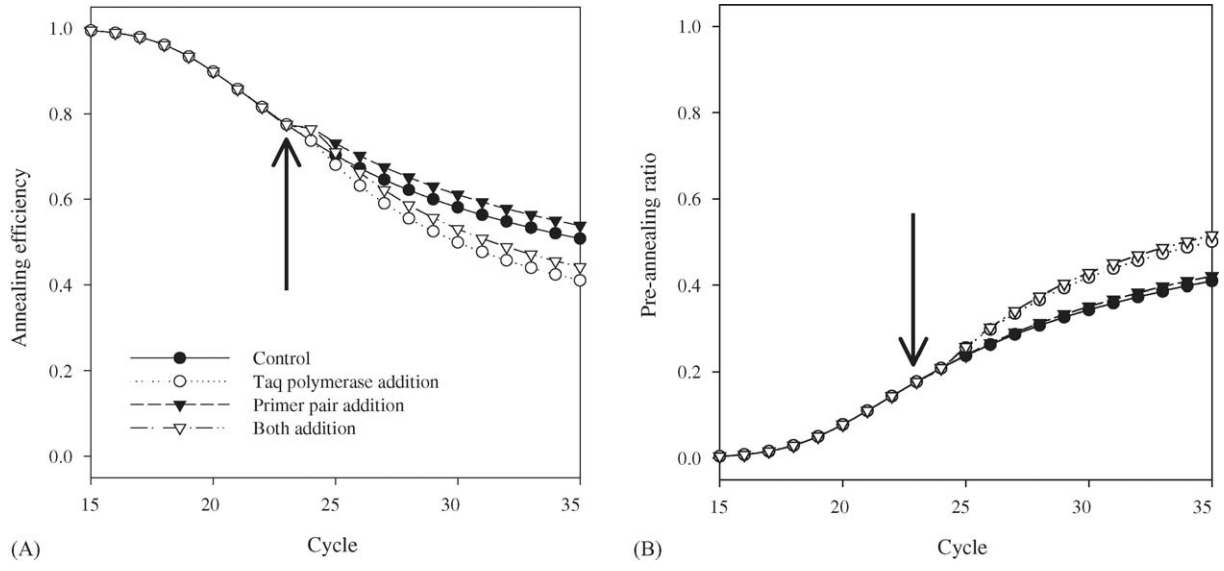

Fig. 6. Simulation results of PCR components addition (*β-actin* fragment). (A) Annealing efficiency. (B) Pre-annealing ratio. (●): control (distilled water addition), (○): *Taq* polymerase addition, (▼): primer pair addition. (▽): *Taq* polymerase and primer pair addition. The arrows indicate the cycle when the components were added.

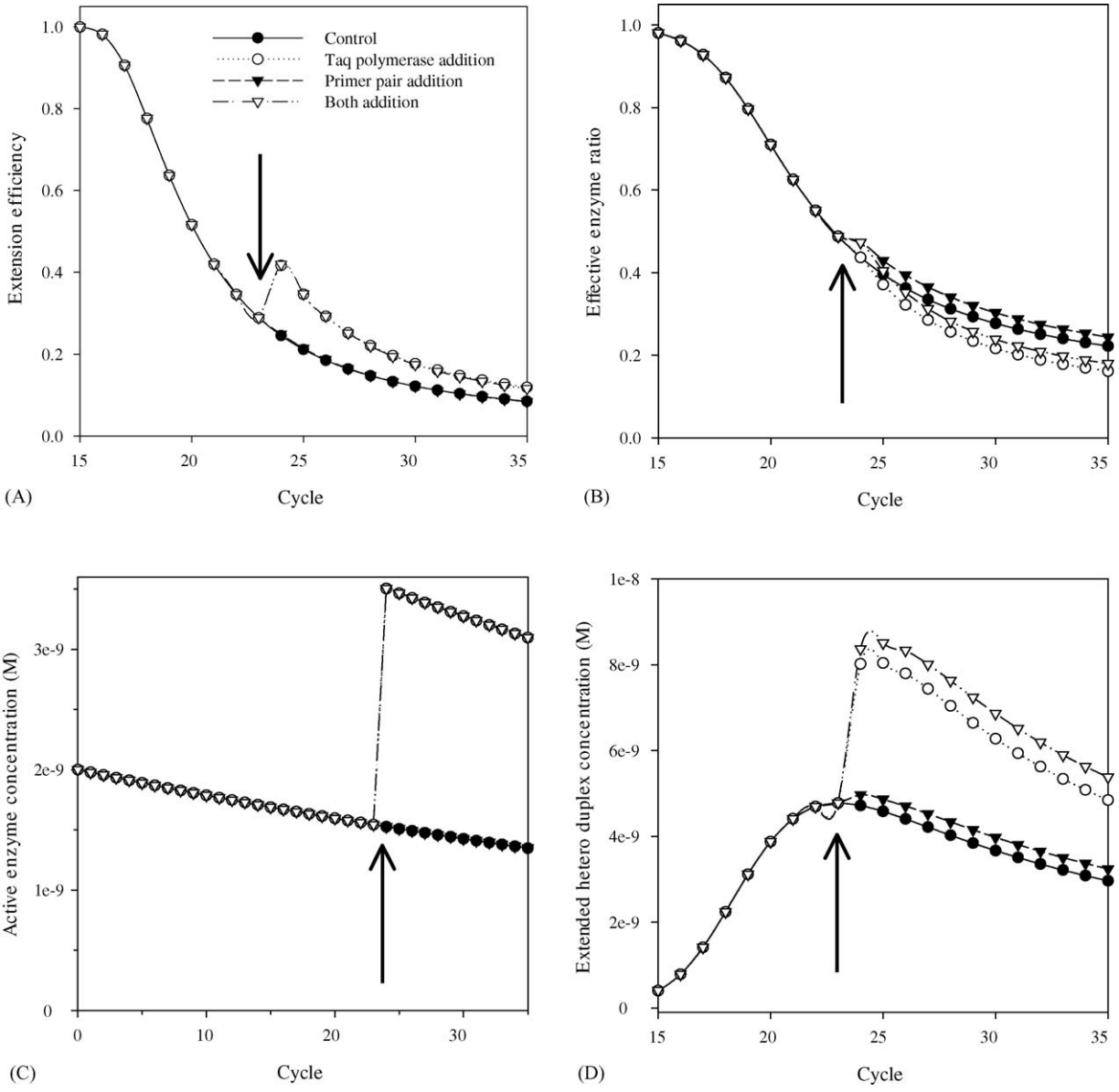

Fig. 7. Simulation results of PCR components addition (*β-actin* fragment). (A) Extension efficiency. (B) Effective enzyme ratio. (C) Active enzyme concentration. (D) Extended hetero duplex concentration. (●): control (distilled water addition), (◯): *Taq* polymerase addition, (▼): primer pair addition, (▽): *Taq* polymerase and primer pair addition. The arrows indicate the cycle when the components added.

The annealing efficiency and pre-annealing ratio change were plotted as shown in Fig. 6. When polymerase was added in the middle of PCR (after 23 cycles) the pre-annealing ratio was increased and the annealing ratio was decreased. The cause of these results was thought to be due to more product accumulation by enhanced extension efficiency (Fig. 7(A)). Polymerase addition significantly increased the extension of primer-template hetero duplexes formed in the annealing step, which is the limiting step in the process (Fig. 7(D)). Though polymerase addition could increase the concentration of effective enzyme, the increased PCR efficiency induced a higher product accumulation, which consequently reduced the annealing efficiency.

Thermal inactivation of polymerase was not so significant and the active enzyme concentration was preserved at 67% of initial concentration at the end of the PCR (Fig. 7(C)). The extension efficiency was dropped dramatically after 15 cycles because of the limited amount of effective enzyme in the mixture (Fig. 7(A) and (B)). The primer-template hetero duplex molecules were not completely extended to fully double-stranded DNA because of the limitation of effective polymerase, so the extension efficiency decreased dramatically after 15 cycles and the quasi-linear phase began.

While primer addition brought about a slight increase in annealing efficiency, there was no noticeable change in the pre-annealing ratio (Fig. 6(A) and (B)). Increase of anneal-

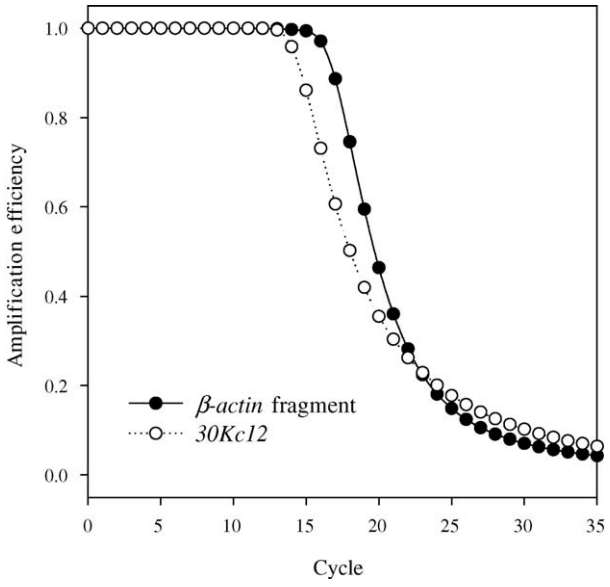

Fig. 8. Simulation results of length effect on amplification profile. Amplification efficiency difference between *β-actin* fragment and *30Kc12*.

ing efficiency generated more hetero-duplexes, and this raised the effective enzyme ratio (Fig. 7(B)). However, the effect of primer addition fell short of expectation, because primer addition could not prevent pre-annealing. Additive primer could only promote the primer-template hetero duplex formation in competitive annealing.

Decrease of annealing efficiency within each cycle can also be explained by the dependency of the melting temperature on the concentration of DNA duplex. The melting temperature of DNA rises as its concentration increases [22]. This can be an important cause of annealing efficiency decrease. With progress in PCR, the template concentration increases significantly and the primer concentration decreases. This causes the increase of melting temperature of template and the decrease of melting temperature between primer and template. As a result, the melting temperature difference increases and consequently the pre-annealing effect will be enhanced.

4.4. Simulation results II: template length effect

Simulation results of two templates, *β-actin* fragment (159 bp) and *30Kc12* (795 bp), were compared to investigate the effect of length of the DNA on the amplification profile. Longer DNA strands required more dNTPs incorporation and the limitation of polymerization capacity appeared earlier (Fig. 8). Therefore, the quasi-linear phase began earlier for a longer template and lasted longer compared to a shorter template because the starting time of the plateau phase is influenced by the accumulated product amount. Moreover, it took more time to reach the concentration level required for the plateau. This effect found from the simulation was consistent with the experimental results (Fig. 2), where the quasi-linear phase of *β-actin* fragment was about 14–15 cycles while that of *30Kc12* was about 18 cycles.

4.5. Simulation results III: temperature ramp effect

As discussed above, pre-annealing, thermal inactivation, and product accumulation affected synergistically on the attenuation of amplification. These inhibiting sub-reactions can be partially overcome by rapid temperature transition. The temperature ramping rate was adjusted from 1.1 to 10 °C/s and the pre-annealing ratio and the effective enzyme ratio was plotted (Fig. 9). The pre-annealing ratio was significantly decreased by increasing the temperature

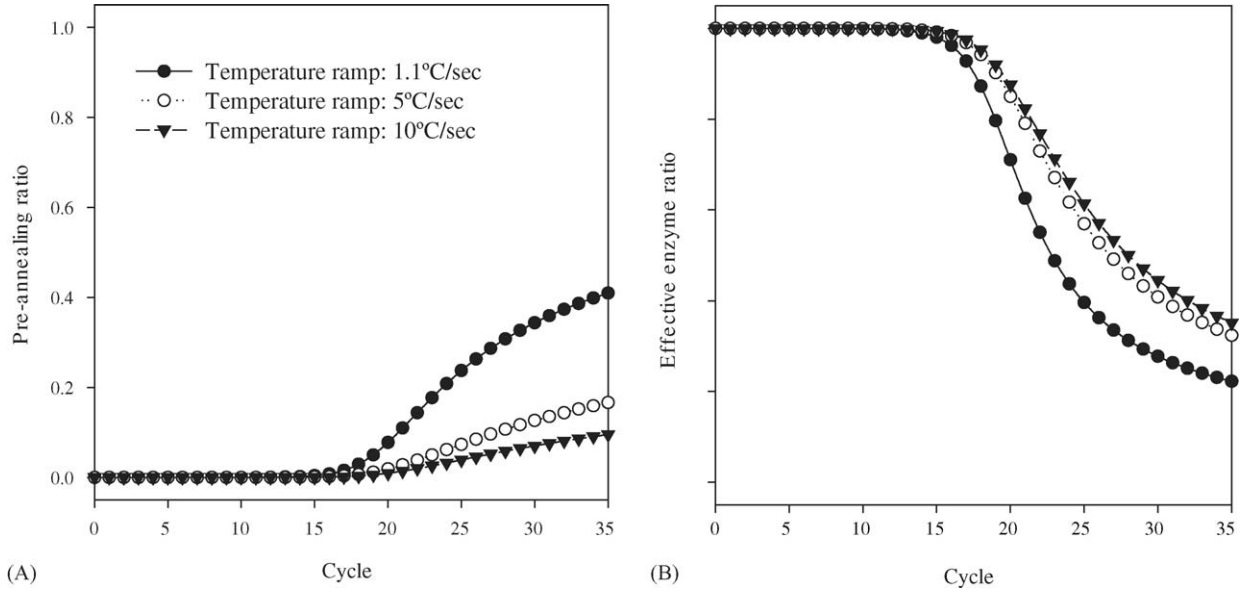

Fig. 9. Simulation results of temperature ramp effect on amplification profile (*β-actin* fragment). (A) Pre-annealing ratio. (B) Effective enzyme ratio. (●): 1.1 °C/s, (◯): 5 °C/s, (▼): 10 °C/s of temperature ramp.

ramp from 1.1 to 5 °C/s while effective enzyme ratio was increased.

Increase of temperature ramp from 5 to 10 °C/s also showed improvement in both ratios, but the extent was insignificant when compared to the improvement in case of a temperature ramp change from 1.1 to 5 °C/s. This is probably because of the difference in pre-annealing time. The final product amount was increased by 31.45% with a temperature ramp of 5 °C/s and by 38.98% with 10 °C/s.

5. Conclusion

We investigated the PCR amplification profile, and especially focused on the plateau phenomenon by monitoring and analyzing the PCR profile after addition of possible reaction limiting components. Simulations were also performed enabling us to have a microscopic view on the amplification process. The addition of polymerase and primer pair led to the increase of the PCR product amount; however the plateau was still observed. This could be explained by the decrease of annealing efficiency resulting from the increase of pre-annealing during temperature transition and the decrease of effective polymerase concentration resulting from the PCR product accumulation. The effects of template length and temperature ramping rate were also analyzed and compared to simulations. Though the plateau phase was the inevitable result of PCR, we could delay the PCR plateau and increase the final product amount by adding essential components. The described model may not be suitable for an actual case, which includes the formation of PCR by-product such as primer-dimers. However, the possibilities of primer-dimer or non-specific PCR product formation can be reduced considerably by designing rational primer pairs using useful software tools.

Acknowledgements

This research was supported by the nanotechnology research fund from the Korean Ministry of Science and Technology and by the MEC Project from the Korean Ministry of Commerce, Industry and Energy. Authors would like to thank Prof. Danny van Noort for his kind advice on this manuscript.

References

[1] R. Saiki, S. Scharf, F. Faloona, K. Mullis, G. Horn, H. Erlich, Enzymatic amplification of β-globin genomic sequences and restriction site analysis for diagnosis of sickle cell anemia, Science 230 (1985) 1350–1354.
[2] R. Saiki, D. Gelfand, S. Stoffel, S. Scharf, R. Higuchi, G. Horn, K. Mullis, H. Erlich, Primer-directed enzymatic amplification of DNA with a thermostable DNA polymerase, Science 239 (1988) 487–491.
[3] J.Y. Lee, J.J. Kim, T.H. Park, Miniaturization of polymerase chain reaction, Biotechnol. Bioprocess Eng. 8 (2003) 213–220.
[4] K.-S. Yun, E. Yoon, Microfluidic components and bio-reactors for miniaturized bio-chip applications, Biotechnol. Bioprocess Eng. 9 (2004) 86–92.
[5] J. Min, J.-H. Kim, S. Kim, Microfluidic device for bio analytical systems, Biotechnol. Bioprocess Eng. 9 (2004) 100–106.
[6] P. Kainz, The PCR plateau phase-towards an understanding of its limitations, Biochim. Biophys. Acta 1494 (2000) 23–27.
[7] C. Morrison, F. Gannon, The impact of the PCR plateau phase on quantitative PCR, Biochim. Biophys. Acta 1219 (1994) 493–498.
[8] S. Schnell, C. Mendoza, Theoretical description of the polymerase chain reaction, J. Theor. Biol. 188 (1997) 313–318.
[9] S. Schnell, C. Mendoza, Enzymological considerations for a theoretical description of the quantitative competitive polymerase chain reaction (QC-PCR), J. Theor. Biol. 184 (1997) 433–440.
[10] J.T. Hsu, S. Das, S. Mohapatra, Polymerase chain reaction engineering, Biotechnol. Bioeng. 55 (1997) 359–366.
[11] A.L. Hayward, P.J. Oefner, S. Sabatini, D.B. Kainer, C.A. Hinojos, P.A. Doris, Modeling and analysis of competitive RT-PCR, Nucl. Acids Res. 26 (1998) 2511–2518.
[12] F. Sun, The polymerase chain reaction and branching processes, J. Comp. Biol. 2 (1995) 63–86.
[13] G. Weiss, A. Haeseler, A coalescent approach to the polymerase chain reaction, Nucl. Acids Res. 25 (1997) 3082–3087.
[14] M.V. Velikanov, R. Kapral, Polymerase chain reaction: A markov process approach, J. Theor. Biol. 201 (1999) 239–249.
[15] G. Stolovitzky, G. Cecchi, Efficiency of replication in the PCR, Proc. Natl. Acad. Sci. U.S.A. 93 (1996) 12947–12952.
[16] S.E. Whitney, A. Sudhir, R.M. Nelson, H.J. Viljoen, Principles of rapid polymerase chain reactions: mathematical modeling and experimental verification, Comput. Biol. Chem. 28 (2004) 195–209.
[17] J.Y. Lee, S.-Y. Shin, B.-T. Zhang, T.H. Park, Solving traveling salesman problems with DNA molecules encoding numerical values, Biosystems 78 (2004) 39–47.
[18] J.-Y. Wang, K. Drlica, Modeling hybridization kinetics, Math. Biosci. 183 (2003) 37–47.
[19] P. Kainz, A. Schmiedlechner, H.B. Strack, Specificity-enhanced hot-start PCR: Addition of double-stranded DNA fragments adapted to the annealing temperature, BioTechniques 28 (2000) 278–282.
[20] S.C. Mohapatra, J.T. Hsu, Kinetics of deactivation for thermostable DNA polymerase enzymes, Biotechnol. Techniq. 10 (1996) 569–572.
[21] D.H. Gelfand, T.J. White, Thermostable DNA polymerase, in: M.A. Innis, D.H. Gelfand, J.J. Sninsky, T.J. White (Eds.), PCR protocols, a guide to methods and applications, Academic Press, San Diego, CA, 1990, pp. 129–141.
[22] P.N. Borer, B. Dengler, I. Tinoco Jr., O.C. Uhlenbeck, Stability of ribonucleic acid double-stranded helices, J. Mol. Biol. 86 (1974) 843–853.